www.amlett.com, www.vbripress.com/aml, DOI: 10.5185/amlett.2015.5821 Published online by the VBRI Press in 2015

Fabrication and characterization of SWCNT-reinforced polyester nanocomposites using tensile test and nanoindentation techniques

Minh-Tai Le[1] and Shyh-Chour Huang[2*]

[1]*Faculty of Mechanical Engineering, Ho Chi Minh City University of Technology and Education, Ho Chi Minh City, Vietnam*
[2]*Department of Mechanical Engineering, National Kaohsiung University of Applied Sciences, Kaohsiung, 80778 Taiwan*

[*]Corresponding author. Tel: (+886) 73814526; Fax: (+886) 73831373; E-mail: shuang@cc.kuas.edu.tw

Received: 25 January 2015, Revised: 13 May 2015 and Accepted: 17 June 2015

ABSTRACT

The main objective of this work is to conduct a manufacturing experiment on a single-walled carbon nanotube (SWCNT)/polyester nanocomposite for characterization of its mechanical properties using a tensile test and nanoindentation techniques. Experimental specimens were made under identical conditions using the hot press process. Dispersion of SWCNTs in an unsaturated polyester matrix was conducted by a sonication method, and a high-speed shear mixer was used for mixing the curing agent and resin. Following the manufacturing of the SWCNT/polyester nanocomposites, characterization of the mechanical properties of the material was performed by tensile testing and nanoindentation techniques. In addition, the morphologies of the fractured surface of SWCNT/polyester nanocomposites were observed with a scanning electron microscope (SEM). The results of mechanical tests exhibit improvements of Young's modulus and hardness by 35% and 29%, respectively, at 1.0 wt% SWCNTs. In addition, the elastic modulus determined by the nanoindentation technique differs from the one obtained from tensile tests by 16%. The experimental samples are expected to yield the novel promising materials that offer a low-cost, high-strength material for use in the manufacture of lightweight components for automobiles, transportation systems and consumer products.

Keywords: Single-walled carbon nanotube (SWCNT); unsaturated polyester; nanocomposite; tensile test; nanoindentation.

Introduction

Carbon nanotubes (CNTs) [**1**] have excellent mechanical and electrical properties, and are also good reinforcing materials for composites. Zeng *et al.* [**2**] found an increase of 50% in Young's modulus of CNT-reinforced PMMA composites with 5% of carbon nanotubes. Rio *et al.* [**3**] presented that the yield stress and Young's modulus of CNT based PET increased 6.5% and 11.9%, respectively, when 0.3% of CNTs were added into PET. Carbon nanotubes are suitable for reinforcement of a variety of polymer matrices, such as polyamides, epoxy, polypropylene and polyester. Among them, polyester is the most commonly used polymer matrix for nanocomposite materials, due to its low cost and variety of applications in transportation and the production of consumer goods [**4**]. Unsaturated polyester resin possesses very good mechanical, thermal and corrosion- resistant properties, and is also simpler and less costly than epoxy. Moreover, due to its excellent bonding, thermal, mechanical, dielectric and aging characteristics [**5, 6**], polyester resins have a wide range of industrial relevance. They are used in industrial finishes and maintenance, have architectural uses, and are used in paints and surface coatings. Shokrieh *et al.* [**7**] investigated the mechanical properties of multi-walled carbon nanotube/polyester nanocomposites. A.K. Dutta et al. [**8**] recently presented nanoindentation testing for evaluating the modulus and hardness of single-wall carbon nanotube- reinforced epoxy composites.

Nanoindentation testing provides a successful technique for studying the mechanical properties of these nanomaterials at very low load. To better understand these properties [**10**], earlier literature describes some experimental works on the nanoindentation of Nylon 11/clay nanocomposites [**9**] and clay/poly (ethylene oxide) nanocomposites. Although CNT/polymer composites have been investigated in numerous studies, there are only a few on CNT/polyester composites. In particular, single-walled carbon nanotube reinforced polyester nanocomposites have been rarely discussed in previous literature.

In this study, experiments specifically designed to characterize the mechanical properties of SWCNT/polyester nanocomposites were conducted. The experimental specimens were made under identical conditions using a hot-pressing process. Following this fabrication, the tensile test and nanoindentation techniques were used to characterize the mechanical properties of SWCNT/polyester nanocomposites. Scanning electron microscopy (SEM) was employed to determine the

dispersion state of CNTs in the matrix, as well as the fracture surface properties. The novelty of the current study is that the reinforced polyester materials were manufactured as unique, low-cost, high strength materials to be used in manufacturing lightweight components for automobile parts, transportation systems and consumer products.

Experimental

Materials

The single-walled carbon nanotubes (**Fig. 1**) used in this study were grown by chemical vapor deposition with outer diameters between 1 to 4 nm and inner diameters between 0.8 to 1.6 nm, and purified to > 99%; they were purchased from Cheaptube.com (USA). Young's modulus was 1 TPa, and expected elongation to failure was 20-30% [**11**]. The unsaturated polyester resin was supplied by Golden Innovation Business Co. (Taiwan) and was cured with Cobalt naphthenate (6%) and MEKP, as recommended by the manufacturer.

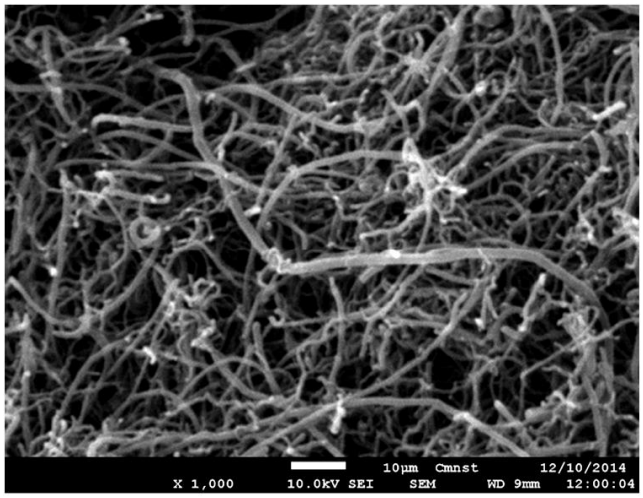

Fig. 1. Scanning electron microscope of MWCNTs.

Preparation of nanocomposites

After several trials, the following procedure was used in the fabrication of the SWCNT/polyester nanocomposites. The amount of SWCNTs and unsaturated polyester was calculated and then mixed together in a beaker. First, SWCNT powder of differing weight percentages (0, 0.5 and 1 wt%) were dispersed in a solvent (chloroform) for 1 h in an ultrasonicator bath (50 kHz). Unsaturated polyester resin was then added to the nanotube-solvent solution and mixed thoroughly with a magnetic stirrer for about 60 min at 60^0C until most of the solvent had evaporated. Then the mixture was sonicated for 90 min using a pulse mode (9 s on/ 9 s off) to separate the aggregation of the SWCNTs and to achieve good dispersion. Once this process was completed, hardener/accelerator/catalyst (100:1/1/1 parts by weight) was added to the previously modified mixture. The mixed compound was then placed in a vacuum chamber for about 30 min to remove bubbles. An aluminum mold (**Fig. 2**(**a**)) of the required dimensions was used to make the samples. The mold was coated with a releasing agent to enable easy removal of the sample. The nanocomposite mixture was poured into the mold to fabricate the test specimen, as shown in **Fig. 2(b)**. The closed mold was kept under a pressure of 0.7 MPa for 24 h at room temperature. To ensure a complete curing process, the nanocomposite samples were put into a heat oven and post cured at 80^0C for 3 h. The test specimens were cut to the required sizes from the sample sheet using a Water Jet Cutter with ASTM standard.

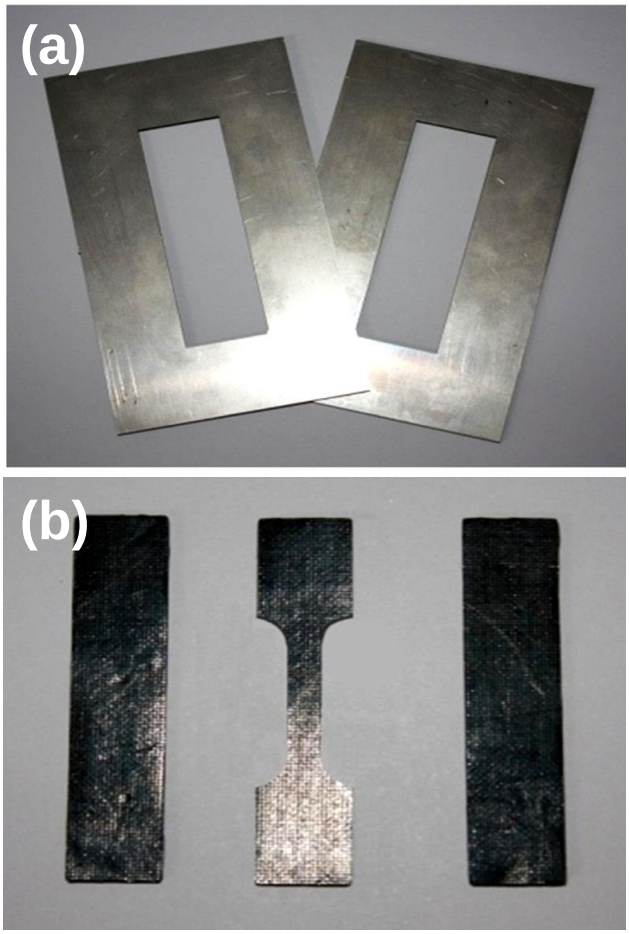

Fig. 2. Mould (a) and nanocomposite specimens; (b) after preparation procedure.

Fig. 3. Tensile tester.

Tensile test

The experimental tensile strength testing was performed on the tensile test machine Instron 5566-CN2081 (Instron Company, Taiwan) (**Fig. (3)**) with an ASTM D638 Type V

standard [**12**]. The parameters for setting up the experiment were as follows: Clamp length: 26.3 mm, tensile speed: 0.5 mm/min, room temperature: 25^0C. In order to obtain a reliability of 95%, at least 5 specimens were tested for each of the filler ratios.

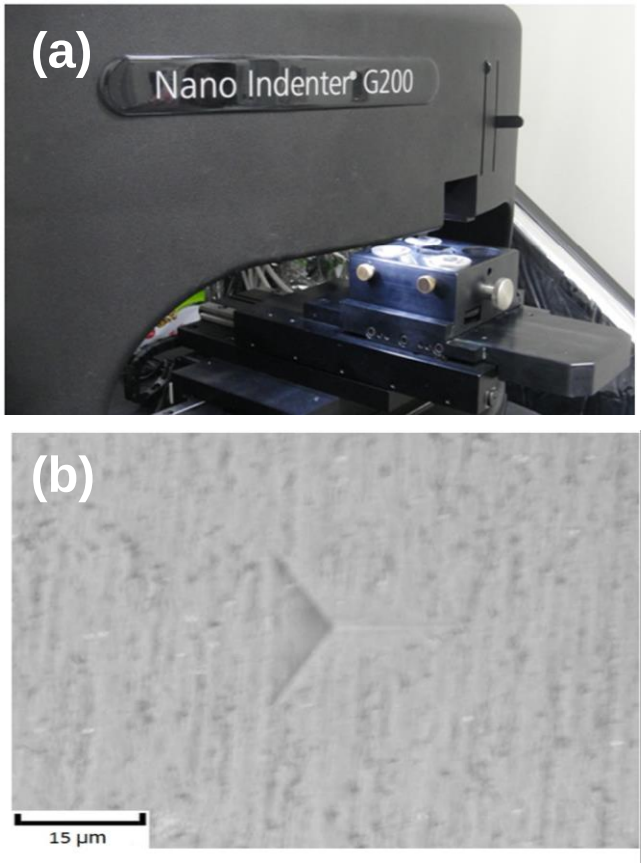

Fig. 4. (a) MTS-G200 Nanoindenter; (b) SEM image of the indenter shape in the specimen.

Nanoindentation test

The elastic modulus and hardness of the casted specimens were obtained from nanoindentation testing using a MTS-G200 Nanoindenter (**Fig. 4a**) with a pyramid-shaped Berkovich indenter (**Fig. 4b**).

Procedure used to calculate the elastic modulus and hardness

The plastic strain rate is determined by consistency with the yield condition.

$$\bar{\sigma} = \sigma_y(e^p) \qquad \text{---------- (1)}$$

where $\bar{\sigma}$ is the effective stress; the yield stress σ_y was chosen here as a simple monotonic function of the cumulative effective plastic strain.

$$e^p = \int \dot{e}^p dt \qquad \text{---------- (2)}$$

in which $\dot{e}^p$ = the scalar effective plastic strain rate and the direction of flow is coaxial with the deviatoric stress.

A schematic representation of nanoindentation is shown in **Fig. 5(a)**. Elastic modulus and hardness values were interpreted from the simulated data based on the composite response of the indenter and the material using the procedure of Oliver *et al.* [**13**]. The loading part of the curve was a combination of elastic and plastic deformation, while the unloading curve was mainly dominated by elastic deformation shown as **Fig. 5(b)**.
Fitting the unloading portion:

$$P = \alpha(h - h_f)^m \qquad \text{---------- (3)}$$

where h_f is the final depth after complete unloading; α, m are fitting parameters determined from regression analysis of the initial stage of the unloading process; P, h were taken from unloading curve.

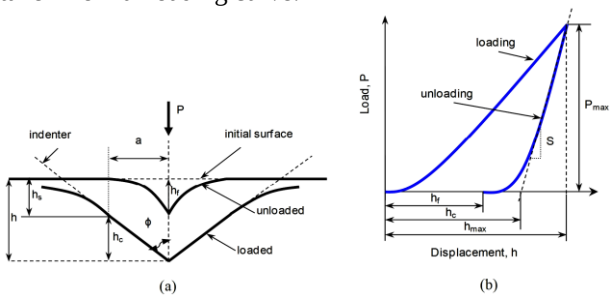

Fig. 5. (a) Schematics of nanoindentation with a Berkovich indenter (b) Load-displacement curve and parameters.

Slope of the unloading curve (Contact stiffness) at the maximum indentation depth:

$$S = \left.\frac{dP}{dh}\right|_{h=h_{\max}} = \alpha m(h_{\max} - h_f)^{m-1} \qquad \text{---------- (4)}$$

where $h_{\max}$ is maximum depth.

Contact indentation depth h_c:

$$h_c = h_{\max} - \varepsilon \frac{P_{\max}}{S} \qquad \text{---------- (5)}$$

in which P_{max} is maximum load at h_{max}, ε is a geometric constant $\varepsilon = 0.75$ for a pyramidal indenter.
Contact area A_c can be expressed as a function of the contact indentation depth as:

$$A_c = 3\sqrt{3}h_c^2 \tan^2 63.5 = 24.5h_c^2 \qquad \text{---------- (6)}$$

The reduced modulus:

$$E_r = \frac{\sqrt{\pi}}{2\beta}\frac{S}{\sqrt{A_c}} \qquad \text{---------- (7)}$$

where β is a constant that depends on the geometry of the indenter. For the Berkovich indenter β = 1.034. The specimen elastic modulus (E_s) can then be calculated as:

$$\frac{1}{E_r} = \frac{1-\upsilon_s^2}{E_s} + \frac{1-\upsilon_i^2}{E_i} \quad \text{---------- (8)}$$

in which $E_{i,s}$, and $\upsilon_{i,s}$ are the elastic modulus and Poisson's ratio, respectively, for the indenter and the specimen. For a diamond indenter, E_i is 1140 GPa and υ_i is 0.07.

Nanoindentation hardness:

$$H = \frac{P_{\max}}{A_c} \quad \text{---------- (9)}$$

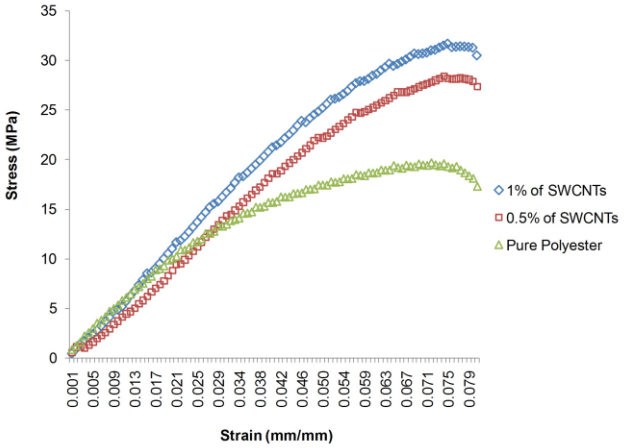

Fig. 6. Stress-strain curve in tensile test for nanocomposite.

Table 1. Results from tensile test.

SWCNT content (%)	Strain at break (%)	Stress at maximum load (MPa)	Modulus (GPa)
0	9.28	16.5	2.95
0.5	4.55	24.8	4.01
1	3.86	32.9	4.13

Results and discussion

Tensile behavior of nanocomposite

The stress-strain curves of the nanocomposites under tension are shown in **Fig. 6**. This figure shows that the tensile properties of the samples with different filler ratios are very similar. At the beginning stage of the tensile test, stress increases gradually in a linear pattern, showing the elastic deformation stage of the material. After that, the tensile stress reaches a maximum value and then decreases rapidly to the completely destroyed stage. The specimens revealed a characteristic elastoplastic and slightly brittle behavior. **Table 1** summarizes the results from one set of such tensile test data. Young's modulus values showed a remarkable increase for 1.0 wt% specimens.

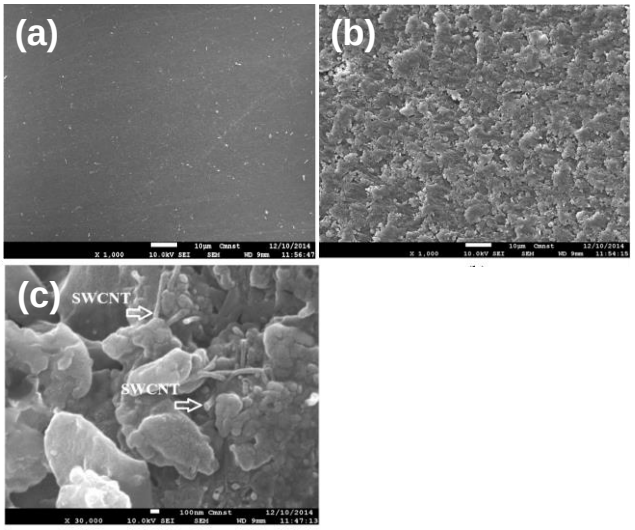

Fig. 7. SEM micrograph of typical fracture surfaces of (a) pure polyester resin; (b) Polyester/SWCNT-1wt% nanocomposite with magnification of 1,000; (c) Polyester/SWCNT-1wt% nanocomposite with magnification of 30,000.

Morphology of fracture surface of specimens in a tensile test

The fracture surfaces of the tensile specimens were examined using a scanning electron microscope (SEM). The pure polyester resin samples displayed a smooth surface, as shown in **Fig. 7(a)**. **Fig. 7(b)** shows the fracture surface of nanocomposites with 1 wt% of SWCNTs, and indicates a rather rough surface and a brittle type of fracture. In the SEM image with 30,000 times magnification as shown in **Fig. 7(c)**, the surface of SWCNTs is seen to be completely covered by polyester resin, which exhibits good adhesion between the SWCNTs and polyester, and explains the better mechanical properties of the resulting SWCNT/polyester nanocomposites.

Nanoindentation behavior of nanocomposite

A series of 5 indents was performed for each sample. The peak load of the indenter was adjusted to maintain loading, unloading and holding times. To avoid the influences of creep behavior on the unloading curve used to obtain the elastic modulus and hardness of the nanocomposite, an optimum peak load holding time of 10 s was selected (**Fig. 8(a)**). The first stage is an approach stage of the indenter to the surface of specimen. Following this, the loading stage was applied at a constant rate of 150μN/s with the load continuously increased to the maximum value of 4.651mN. **Fig. 8(b)** illustrates the typical load-displacement curves of indentations done at a peak indentation load of 4.651 mN on the 1 wt% SWCNT reinforced polyester nanocomposites. No specimen failures were generated during indentation, and no creases or interruptions were found on the unloading curve used to obtain the elastic modulus and hardness of material. The next stage of nanoindentation testing was a holding stage of 10 s followed by an unloading stage. The experiment was complete when the entire applied load had been removed.

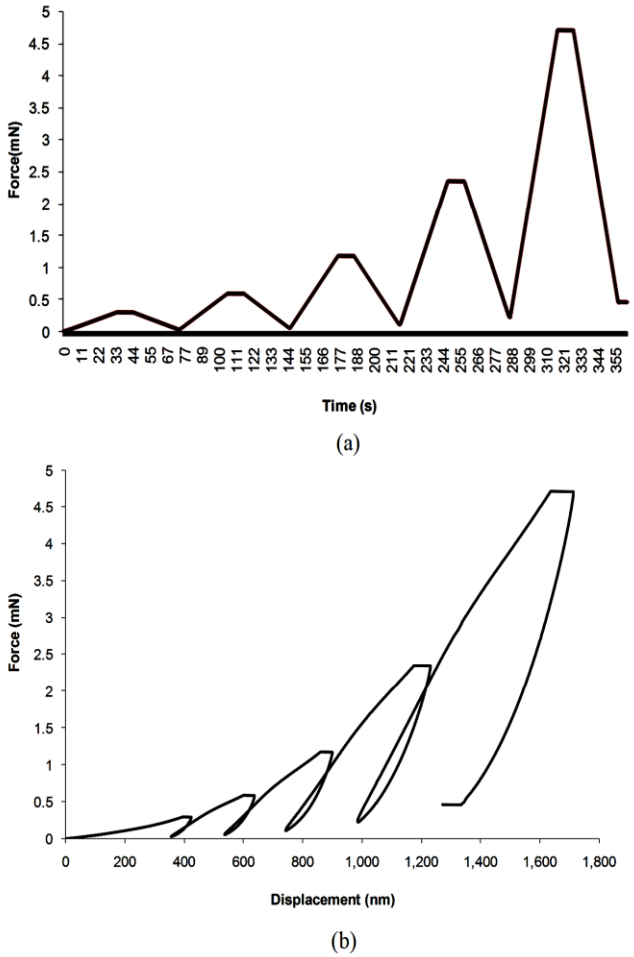

Fig. 8. (a) Loading sequence for a holding time of 10 s (b) Load vs. deformation for 1% by weight SWCNTs reinforced polyester composites.

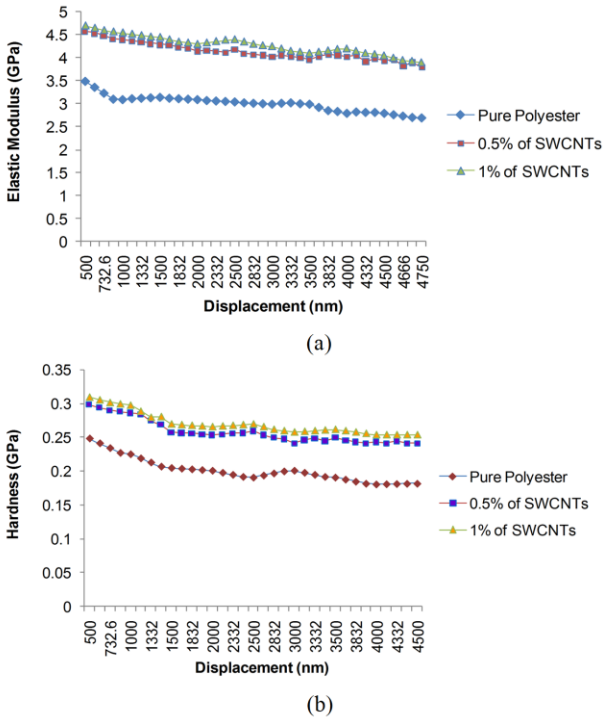

Fig. 9. (a) The variation of the elastic modulus with the depth of indentation; (b)The variation of the hardness with the depth of indentation.

Subsequently, as investigated by other researchers [**14-16**], a depending calculation procedure was utilized for the determination of mechanical properties using Equations (**3-9**). A major variation trend of elastic modulus values in indentation testing is that they will be continuously decreased with an increase of indentation depth for all specimens, as shown in **Fig. 9(a)**. This phenomenon can be explained by the segregation of nanotubes on the surface of the specimen during the sample fabrication process. The decrease in modulus with the increase in depth of nanoindentation could be due to the segregation of nanotubes on the surface of the specimen during the specimen preparation process. Clearly, the elastic modulus of SWCNTs nanocomposites shows an increase, as tested by both the tensile test and the nanoindentation experiment.

Fig. 9(b) shows the variation trend of the hardness of nanocomposites as a function of SWCNT weight percentages. In agreement with the previous outcome, hardness also varies with the elastic modulus, and increases as the weight percentage of SWCNTs increases from 0.5 wt% to 1 wt%. As the carbon nanotubes themselves have greater hardness than those composed of polyester resin, this clarifies the small increase of hardness noted in the 0.5% SWCNT reinforced nanocomposites. It can be concluded that the elastic modulus and hardness increase as the fraction of SWCNTs is increased. Specifically, nanocomposite samples with 1 wt% SWCNT content show an increase of 35% in modulus when compared to the pure polyester sample. Similarly, an increase of 29% in hardness is observed for composites with 1 wt% SWCNT content.

However, a noticeable difference in elastic modulus was obtained from the nanoindentation experiments as compared to the tensile tests, as shown in **Table 2**. Clearly with the nanoindentation testing technique, the elastic modulus obtained was 12-16% higher than the one obtained from the tensile tests. In addition, the reduced elastic modulus values shown in **Table 2** are very close to the elastic modulus values obtained from the uniaxial tensile tests.

Table 2. Elastic moduli values as derived from experiments.

SWCNT content (%)	$E_{tensile}$ (GPa)	$E_{nanoindentation}$ (GPa)	$E_{modified}$ (GPa)	Hardness (GPa)
0	2.95±0.10	3.42±0.10	3.11	0.24
0.5	4.01±0.12	4.57±0.15	4.16	0.30
1	4.13±0.16	4.62±0.20	4.20	0.31

Conclusion

This paper describes how a single-walled carbon nanotube-reinforced polyester nanocomposite was successfully fabricated, and how tensile tests and nanoindentation experiments were conducted to determine the mechanical properties (elastic modulus and hardness) of the nanocomposite material. The variations in modulus and hardness of nanocomposite specimens were evaluated as a function of indentation depth. Polyester reinforced with 1 wt% of SWCNTs showed an increase in the modulus and hardness values of 35% and 29%, respectively, as compared to those of the pure polymer specimen in nanoindentation tests. Moreover, the elastic modulus

determined by the nanoindentation technique differed by 16% from the modulus obtained from tensile tests. In addition, with the SEM images of the tensile fracture surface of SWCNTs/polyester nanocomposites, a good adhesion between the SWCNTs and the resin can be observed. The novelty of the current study is a demonstration that reinforced polyester materials offering both low-cost and high strength can be manufactured to provide lightweight components for automobile parts, transportation systems and consumer products.

Reference

1. Iijima, S.; Helical microtubules of graphitic carbon, *Nature*, **1991**, *354*, 56. **DOI:** 10.1038/354056a0
2. Zeng, J.; Saltysiak, B.; Johnson, W.S.; Schiraldi, D.A.; Kumar, S.; *Composites Part B: Eng. J.* **2004**, *35*, 173. **DOI:** 10.1016/S1359-8368(03)00051-9
3. Rio, T.G.; Poza, P.; Rodriguez, J.; Gutierrez, M.C.G.; Hernandez, J.J.; Ezquerra, T.A.; *Comp. Sci. Technol.* **2010**, *70*, 284. **DOI:** 10.1016/j.compscitech.2009.10.019
4. Cherian, A.B.; Varghese, L.A.; Thachil, E.T.; *Eur. Polym. J.* **2007**, *43*, 1460. **DOI:** 10.1016/j.eurpolymj.2006.12.041
5. Li, J.; Guo, Z.J. *Polym. Plastics Technol. Eng.* **2011**, *50*, 996. **DOI:** 10.1080/03602559.2011.553869
6. Chinnakkannu, K.C.; Muthukaruppan, A.; Josephine, S.R.; Periyannan, G.; *J. Polym. Res.* **2007**, *14*, 319. **DOI:** 10.1007/s10965-007-9114-x
7. Shokrieh, M.M.; Saeedi, A.; Chitsazzadeh, M.; *J. Nanostruct. Chem.* **2013**, 3, 20. **DOI:** 10.1186/2193-8865-3-20
8. Dutta, A.K.; Penumadu, D.; Files, B.; *J. Mat. Res.* **2004**, *19*, 158. **DOI:** 10.1557/jmr.2004.19.1.158
9. Hu, Y.; Shen, L.; Yang, H.; Wang, M.; Liu, T.; Liang, T.; Zhang, J.; *Polym. Testing*, **2006**, *25*, 492. **DOI:** 10.1016/j.polymertesting.2006.02.005
10. Beake, B.D.; Chen, S.; Hull, J.B.; Gao, F.; *J. Nanosci. Nanotechnol.* **2002**, *2*, 73. **DOI:** 10.1166/jnn.2002.077
11. Zhu, J.; Kim, J.; Peng, H.; Margrave, J.L.; Khabashesku, V.N.; and Barrera, E.V.; *Nano Lett.* **2003**, *3*, 1107. **DOI:** 10.1021/nl0342489
12. ASTM D638: Standard Test Method for Tensile Properties of Polymer Matrix Composite Materials. **DOI:** 10.1520/D0638-10
13. Oliver, W.C.; Pharr, G.M.; *J. Mat. Res.* **2004**, *19*, 3-20. **DOI:** 10.1557/jmr.2004.19.1.3
14. Briscoey, B.J.; Fiori, L.; Pelillo, E.; *J. Phys. D: Appl. Phys.* **1998**, *31*, 2395. **DOI:** 10.1088/0022-3727/31/19/006
15. Ayatollahi, M.R.; Doagou-Rad, S.; Shadlou, S.; *Macromol. Mat. Eng.* **2012**, *297*, 689. **DOI:** 10.1002/mame.201100271
16. Shokrieh, M.M.; Hosseinkhani, M.R.; Naimi-Jamal, M.R.; Tourani, H.; *Polym. Testing*, **2013**, *32*, 45. **DOI:** 10.1016/j.polymertesting.2012.09.001

